Nuclear Mathematical and Computational Sciences: A Century in Review, A Century Anew
Gatlinburg, Tennessee, April 6-11, 2003, on CD-ROM, American Nuclear Society, LaGrange Park, IL (2003)

A RESIDUAL MONTE CARLO METHOD FOR THERMAL RADIATION DIFFUSION

T.M. Evans, T.J. Urbatsch, H. Lichtenstein, J.E. Morel
Los Alamos National Laboratory
CCS–4, MS D409 Los Alamos, NM, 87545
tme@lanl.gov; tmonster@lanl.gov; hal@lanl.gov; jim@lanl.gov

ABSTRACT

Residual Monte Carlo methods reduce statistical error at a rate of $\exp(-bN)$, where b is a positive constant and N is the number of particle histories. Contrast this convergence rate with $1/\sqrt{N}$, which is the rate of statistical error reduction for conventional Monte Carlo methods. Previous research has shown that the application of residual Monte Carlo methods to the solution of continuum equations, such as the radiation transport equation, is problematic for all but the simplest of cases. However, the residual method readily applies to discrete systems as long as those systems are monotone, i.e., they produce positive solutions given positive sources. We develop a residual Monte Carlo method for solving a discrete 1-D non-linear thermal radiative equilibrium diffusion equation, and we compare its performance with that of the discrete conventional Monte Carlo method upon which it is based. We find that the residual method provides efficiency gains of many orders of magnitude. Moreover, fully consistent non-linear solutions can be obtained in a reasonable amount of time because of the effective absence of statistical noise. We conclude that the residual approach has great potential and that further research into such methods should be pursued for more general discrete and continuum systems.

Key Words: residual Monte Carlo, thermal radiation, diffusion

1. INTRODUCTION

Monte Carlo methods are commonly used to simulate radiation transport phenomena. The overwhelming majority of these methods are constrained by the Central Limit Theorem. Thus, convergence in these methods is limited to $1/\sqrt{N}$, where N is the number of particle histories.

Halton [1] has shown that a Monte Carlo method based upon a residual approach could be used to solve certain matrix equations. The exciting aspect of this work was that exponential convergence was obtained; the statistical error was proportional to $\exp(-bN)$. This work has not been disseminated widely in the transport community.

Over the last several years, researchers at Los Alamos National Laboratory have applied residual Monte Carlo methods to radiation transport calculations with the intent of demonstrating exponential convergence for continuum systems [2–6]. While they were able to demonstrate exponential convergence for simple, homogeneous, one-speed, 1-D problems, significant difficulties were encountered for simple multidimensional problems. As we will explain later, such difficulties can be expected to arise for a broad class of problems. Presently, the true potential of residual Monte Carlo methods relative to conventional

Monte Carlo methods for solving complex problems of physical interest is not well established; however, we will show that great advantages can be accrued by using residual methods on discrete systems.

The purpose of the present study is to demonstrate that enormous speedups, relative to conventional Monte Carlo, can be obtained using a residual Monte Carlo method to solve a discrete system that *approximates* a continuum system. Most importantly, we show that statistical errors in the solution can be efficiently reduced to negligible levels making it possible to solve a strongly non-linear, discrete system with a fully implicit treatment of the non-linearities. It is essentially impossible to do this with conventional Monte Carlo techniques.

2. THE RESIDUAL MONTE CARLO METHOD

We wish to solve the following linear equation,

$$\hat{A}x = b\,, \tag{1}$$

where $\hat{A}$ is a linear operator, x is the solution, and b is the driving function. Suppose that we have an approximate solution, $\tilde{x}$, to Eq. (1). The error associated with $\tilde{x}$ is defined as follows,

$$\delta\tilde{x} = x - \tilde{x}\,. \tag{2}$$

The error term, $\delta\tilde{x}$, can also be considered a correction term for the approximate solution, $x = \tilde{x} + \delta\tilde{x}$.

Substituting Eq. (2) into Eq. (1) yields

$$\hat{A}\delta\tilde{x} = r\,, \tag{3}$$

where r is the residual and is defined,

$$r = b - \hat{A}\tilde{x}\,. \tag{4}$$

Clearly, any method that solves Eq. (1) can be used to solve Eq. (3). Furthermore, if $\tilde{x} = 0$ then Eq. (3) becomes identical to Eq. (1).

Based upon the previous discussion, we can postulate a residual Monte Carlo algorithm:

1. Start with a solution estimate, $\tilde{x}$.
2. Do a *stage*
   - perform a conventional Monte Carlo calculation to solve Eq. (3) for the correction, $\delta\tilde{x}$.
   - add $\delta\tilde{x}$ to $\tilde{x}$ to obtain a new solution estimate.
3. Run stages until $\tilde{x}$ converges.

This algorithm constitutes the theme of residual Monte Carlo methods.

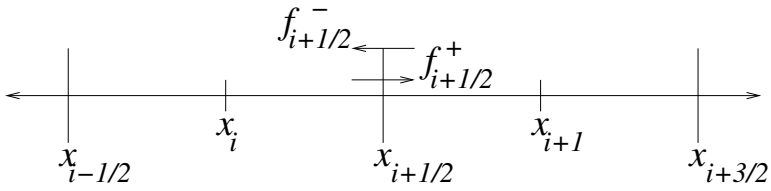

Figure 1. 1-D discretized mesh. We integrate over the cell from $x_{i-1/2}$ to $x_{i+1/2}$.

3. A DISCRETE SCHEME FOR NON-LINEAR THERMAL RADIATIVE DIFFUSION

Consider the gray, equilibrium diffusion equation in the absence of external sources or scattering [7],

$$(C_v + 4aT^3)\frac{\partial T}{\partial t} - \frac{\partial}{\partial x}\frac{4acT^3}{3\sigma_R}\frac{\partial T}{\partial x} = 0\,, \tag{5}$$

where $C_v \equiv C_v(x,T(x,t))$ [jerks $\cdot$ cm$^{-3}\cdot$ keV^{-1}] is the specific heat capacity of the material, $a = 0.01372$ [jerks $\cdot$ cm$^{-3}\cdot$ keV^{-4}] is the radiation constant, $c = 299.79$ [cm $\cdot$ sh^{-1}] is the vacuum light speed, and $T \equiv T(x,t)$ [keV] is the temperature that characterizes both the radiation and the material. The opacity, $\sigma_R \equiv \sigma_R$(x,T(t)) [cm^{-1}], is the Rosseland Mean opacity, and $D \equiv D(x,T(x,t))$ [cm], is the diffusion constant. The equation is non-linear in temperature, both from terms containing T explicitly and implicitly through σ_R and C_v.

In what follows, we shall define Eq. (5) in terms of T^4 instead of T,

$$\Big(\frac{C_v}{4acT^3} + \frac{1}{c}\Big)\frac{\partial \phi}{\partial t} - \frac{\partial}{\partial x}D\frac{\partial \phi}{\partial x} = 0\,, \tag{6}$$

where $\phi \equiv \phi(x,t)$[Jerks $\cdot$ cm$^{-2}\cdot$ sh^{-1}] is the angle-energy integrated radiation intensity. The intensity is $\phi(x,t) = acT^4$ in the *local* thermodynamic equilibrium (LTE) limit.

We wish to formulate a set of discrete probability equations in terms of the face-centered partial fluxes that we can solve using Monte Carlo methods. Casting the equations in terms of the face-centered partial fluxes provides a convenient form for a Monte Carlo scheme because particle flow provides the inter-cell coupling. We begin by applying a backward-Euler method to discretize Eq. (6) in time,

$$\Big(\frac{C_v^n}{4acT^{n\,3}} + \frac{1}{c}\Big)\frac{\phi^{n+1}-\phi^n}{\Delta t} - \frac{d}{dx}D^n\frac{d\phi^{n+1}}{dx} = 0\,. \tag{7}$$

We begin the spatial treatment of the time-discretized equation by considering Fig. 1. Operating on Eq. (7) with $\int_{x_{i-1/2}}^{x_{i+1/2}}(\cdot)dx$ and applying Fick's Law yields

$$\tilde{\sigma}_i^n\phi_i^{n+1}\Delta x + F_{i+1/2}^{n+1} - F_{i-1/2}^{n+1} = \tilde{\sigma}_i^n\phi_i^n\Delta x\,, \tag{8}$$

where

$$\tilde{\sigma}_i^n = \left(\frac{C_v^n}{4acT_c^{n\,3}\Delta t} + \frac{1}{c\Delta t} \right) [\mathrm{cm}^{-1}], \tag{9}$$

$$\phi_i^n = acT_i^{n\,4} \, [\mathrm{jerks} \cdot \mathrm{cm}^{-2} \cdot \mathrm{sh}^{-1}], \tag{10}$$

$$D^n = \frac{1}{3\sigma_{\mathrm{R}}^n} \, [\mathrm{cm}]. \tag{11}$$

Here, $\Delta x = x_{i+1/2} - x_{i-1/2}$, which we will consider constant throughout the mesh for simplicity. Also, F is the face-centered flux in units of $[\mathrm{jerks} \cdot \mathrm{cm}^{-2} \cdot \mathrm{sh}^{-1}]$, defined as the net difference of the right-going and left-going partial fluxes.

Equation (8) is a photon-energy balance equation that states that the photon absorption at time t^{n+1} and the sum of the net outgoing fluxes on the cell-edges is equal to the material radiation emission in the cell at time t^n. To complete the discrete diffusion scheme we need to define expressions for the outgoing partial fluxes in terms of the cell-centered intensities, sources, and incoming partial fluxes.

We can apply forward-differencing to Fick's Law to achieve expressions for the face-centered fluxes,

$$F_{i-1/2}^{n+1} = \frac{-2D^n}{\Delta x}(\phi_i^{n+1} - \phi_{i-1/2}^{n+1}), \tag{12a}$$

$$F_{i+1/2}^{n+1} = \frac{-2D^n}{\Delta x}(\phi_{i+1/2}^{n+1} - \phi_i^{n+1}). \tag{12b}$$

where D^n is evaluated at the cell center. We can use the Marshak boundary condition,

$$4f_{\mathrm{bnd}}^{(\pm)} = \phi(x) + 2D(x)\frac{\partial \phi(x)}{\partial x}\mathbf{n} \cdot \mathbf{i}, \tag{13}$$

to write equations for the incoming partial fluxes. Substituting Fick's Law into Eq (13), we write

$$f_{i-1/2}^{(+)n+1} = \frac{1}{4}\phi_{i-1/2}^{n+1} + \frac{1}{2}F_{i-1/2}^{n+1}, \tag{14a}$$

$$f_{i+1/2}^{(-)n+1} = \frac{1}{4}\phi_{i+1/2}^{n+1} - \frac{1}{2}F_{i+1/2}^{n+1}. \tag{14b}$$

Now, eliminating the cell-edge intensities between Eqs. (12) and (14) and using the definition of the net flux, $F^{n+1} = f^{(+)n+1} - f^{(-)n+1}$, we can write expressions for the outgoing, face-centered, partial fluxes,

$$f_{i+1/2}^{(+)n+1} = \frac{2D^n}{\Delta x + 4D^n}\phi_i^{n+1} + \frac{\Delta x - 4D^n}{\Delta x + 4D^n} f_{i+1/2}^{(-)n+1}, \tag{15a}$$

$$f_{i-1/2}^{(-)n+1} = \frac{2D^n}{\Delta x + 4D^n}\phi_i^{n+1} + \frac{\Delta x - 4D^n}{\Delta x + 4D^n} f_{i-1/2}^{(+)n+1}. \tag{15b}$$

These equations are symmetric because we use a cell-centered diffusion coefficient.

Having defined equations for the outgoing partial fluxes, we now require an expression for the cell-centered intensity, ϕ_i^{n+1}, in terms of the incoming partial fluxes. We can write expressions for the face-centered

fluxes by considering Eqs. (12) and (14),

$$F_{i-1/2}^{n+1} = \frac{8D^n}{\Delta x + 4D^n} f_{i-1/2}^{(+)n+1} - \frac{2D^n}{\Delta x + 4D^n} \phi_i^{n+1}, \tag{16a}$$

$$F_{i+1/2}^{n+1} = \frac{2D^n}{\Delta x + 4D^n} \phi_i^{n+1} - \frac{8D^n}{\Delta x + 4D^n} f_{i+1/2}^{(-)n+1}. \tag{16b}$$

Plugging these equations into the balance equation, Eq. (8), yields the following expression for the cell-centered intensity,

$$\phi_i^{n+1} = \frac{\tilde{\sigma}_i^n \phi_i^n \Delta x + \frac{8D^n}{\Delta x + 4D^n}\left(f_{i-1/2}^{(+)n+1} + f_{i+1/2}^{(-)n+1}\right)}{\tilde{\sigma}_i^n \Delta x + \frac{4D^n}{\Delta x + 4D^n}}. \tag{17}$$

We can substitute Eq. (17) into Eqs. (15); this gives us the following equations for the outgoing, partial fluxes,

$$f_{i+1/2}^{(+)n+1} = P_{\mathrm{T},i} f_{i-1/2}^{(+)n+1} + P_{\mathrm{R},i} f_{i+1/2}^{(-)n+1} + q_{i+1/2}^{(+)n}, \tag{18a}$$

$$f_{i-1/2}^{(-)n+1} = P_{\mathrm{R},i} f_{i-1/2}^{(+)n+1} + P_{\mathrm{T},i} f_{i+1/2}^{(-)n+1} + q_{i-1/2}^{(-)n}. \tag{18b}$$

Here, $P_{\mathrm{T},i}$ is the probability of transmission through cell i, $P_{\mathrm{R},i}$ is the probability of reflection from cell i, and $P_{\mathrm{A},i} = 1 - P_{\mathrm{T},i} - P_{\mathrm{R},i}$ is the probability of absorption in cell i. Because of the symmetry resulting from having a cell-centered diffusion coefficient, the probabilities are the same in both equations. The form for the probability of transmission is

$$P_{\mathrm{T},i} = \frac{4R^2}{\tilde{\sigma}_i^n \Delta x + 2R}, \tag{19}$$

and the probability of reflection is

$$P_{\mathrm{R},i} = 1 - 4R\left(\frac{\tilde{\sigma}_i^n \Delta x + R}{\tilde{\sigma}_i^n \Delta x + 2R}\right), \tag{20}$$

where

$$R = \frac{2D^n}{\Delta x + 4D^n}. \tag{21}$$

The outgoing face-centered sources from each cell are equal in magnitude in this case because of symmetry. The sources are expressed as,

$$\begin{aligned} q_{i+1/2}^{(+)n} &= q_{i-1/2}^{(-)n} \\ &= \frac{2D^n}{\Delta x + 4D^n}\left(\frac{\tilde{\sigma}_i^n \phi_i^n \Delta x}{\tilde{\sigma}_i^n \Delta x + \frac{4D^n}{\Delta x + 4D^n}}\right). \end{aligned} \tag{22}$$

Equations (18) are the fundamental equations of the discrete equilibrium diffusion Monte Carlo (EqDDMC) method [8].

Having defined a set of probability equations for the partial fluxes at each face, we can now describe a conventional Monte Carlo method for solving these equations.

1. Calculate the $P_{\mathrm{R},i}$ and $P_{\mathrm{T},i}$ for each cell.

2. Sample source particles in each cell i with weights,

$$w_i^{(+)} = \frac{q_{i+1/2}^{(+)n} + \frac{1}{2}Q_i^n \Delta x}{N_i^{(+)}}, \tag{23a}$$

$$w_i^{(-)} = \frac{q_{i-1/2}^{(-)n} + \frac{1}{2}Q_i^n \Delta x}{N_i^{(-)}}, \tag{23b}$$

   where the Q_i^n are cell-centered external sources and the N_i are the numbers of plus/minus particles per cell.

3. Stochastically transport particles from cell to cell based on the pre-calculated probabilities for transmission, reflection, and absorption. Tally the $f^{(+)n+1}$ and $f^{(-)n+1}$ on each face. A particle history is terminated when a particle escapes the system or is absorbed.

4. After transporting all particles, use Eq. (17) to calculate ϕ_i^{n+1}, from which we can calculate T^{n+1}.

5. Update material properties and run next timestep until the problem end time is reached.

These steps represent the application of a conventional Monte Carlo algorithm to solve Eqs. (18). In § 4 we will derive the residual form of these equations that will follow the same basic solution procedure illuminated here.

4. A RESIDUAL METHOD FOR NON-LINEAR THERMAL RADIATIVE DIFFUSION

As described in § 2, we can derive a residual method from the conventional Monte Carlo method defined in § 3. Furthermore, the Monte Carlo part of the solution algorithm remains unchanged between the conventional and residual schemes. Equations (18) are solved with discrete Monte Carlo particle transport to get estimates for the partial fluxes, $\tilde{f}^{(+)n+1}$ and $\tilde{f}^{(-)n+1}$, on each face. As shown in Eq. (4) we can use these partial flux estimates to calculate residuals on each face via an application of Eq. (4) to Eqs. (18),

$$r_{i+1/2}^{(+)} = P_{\mathrm{T},i}\tilde{f}_{i-1/2}^{(+)n+1} + P_{\mathrm{R},i}\tilde{f}_{i+1/2}^{(-)n+1} + q_{i+1/2}^{(+)n} - \tilde{f}_{i+1/2}^{(+)n+1}, \tag{24a}$$

$$r_{i-1/2}^{(-)} = P_{\mathrm{R},i}\tilde{f}_{i-1/2}^{(+)n+1} + P_{\mathrm{T},i}\tilde{f}_{i+1/2}^{(-)n+1} + q_{i-1/2}^{(-)n} - \tilde{f}_{i-1/2}^{(-)n+1}. \tag{24b}$$

The partial fluxes on problem boundaries are known; thus, the residuals are on the boundaries are zero, $r_{1/2}^{(+)} = r_{I+1/2}^{(-)} = 0$.

Now, if Eqs. (24) are subtracted from Eqs. (18), we obtain the analog of Eq. (3) for corrections to the partial flux estimates,

$$\delta\tilde{f}_{i+1/2}^{(+)n+1} = P_{\mathrm{T},i}\delta\tilde{f}_{i-1/2}^{(+)n+1} + P_{\mathrm{R},i}\delta\tilde{f}_{i+1/2}^{(-)n+1} + r_{i+1/2}^{(+)}, \tag{25a}$$

$$\delta\tilde{f}_{i-1/2}^{(-)n+1} = P_{\mathrm{R},i}\delta\tilde{f}_{i-1/2}^{(+)n+1} + P_{\mathrm{T},i}\delta\tilde{f}_{i+1/2}^{(-)n+1} + r_{i-1/2}^{(-)}. \tag{25b}$$

Here, $\delta\tilde{f}$ is the correction to the original estimates of the partial fluxes. We can solve for these corrections in the same manner that we solved Eqs. (18). In fact, Eqs. (25) are identical to Eqs. (18) with the exception that the residuals replace the source terms, and we solve for partial flux corrections instead of the partial fluxes.

Equations (18) and (25) imply a residual scheme that is run in stages. Each stage, k, provides a correction to the initial estimates of the partial fluxes,

$$\tilde{f}^{k+1} = \tilde{f}^{k} + \delta\tilde{f}^{k} \,. \tag{26}$$

We now can postulate a residual scheme (REqDDMC) based on these equations:

1. Do a standard, § 3, discrete iteration to solve for $\tilde{f}^{0}$ in the first timestep.
2. Use Eqs. (24) to solve the residuals.
3. Solve Eqs. (25) to get corrections to the partial fluxes, which is equivalent to the EqDDMC transport scheme (Eq. (18)) with a modified source.
4. Use Eq. (26) to update the flux estimates and test for convergence on the partial fluxes.
5. If not converged return to step (2).
6. If converged, calculate T^{n+1} using Eq. (17) and update material properties. Use $\tilde{f}^{(-)n+1}$ and $\tilde{f}^{(+)n+1}$ to calculate the first stage residual for the t^{n+2} timestep. Continue running timesteps until end time is reached.

As we shall show, the great advantage of the residual scheme is that work is only performed where the residuals are high. There is no source in Eqs. (25) where $r \sim 0$. Additionally, using $\tilde{f}^{(-)n+1}$ and $\tilde{f}^{(+)n+1}$ to estimate the residuals in the following timestep means that the costly EqDDMC transport step need only be run in the first stage of the first problem cycle.

5. RESULTS

We have tested the residual EqDDMC method on the non-linear Marshak Wave problem [9]. This 1-D equilibrium problem has an isotropic intensity impinging on a cold, pure-absorbing slab. The problem is solved analytically by assuming that the heat capacity is constant, the opacity follows a power law, and the material energy density dominates the radiative energy density, i.e. $4aT^3 \ll C_v$. The Marshak wave problems solved below have the following parameters:

$$C_v = 0.1 \ [\text{Jerks} \cdot \text{g}^{-1} \cdot \text{keV}^{-1}]$$
$$\sigma = \frac{100}{T^3} \ [\text{cm}^{-1}]$$
$$f_{\text{left}}^{(+)} = \frac{ac}{4} \ [\text{Jerks} \cdot \text{cm}^{-2} \cdot \text{s}^{-1}]$$

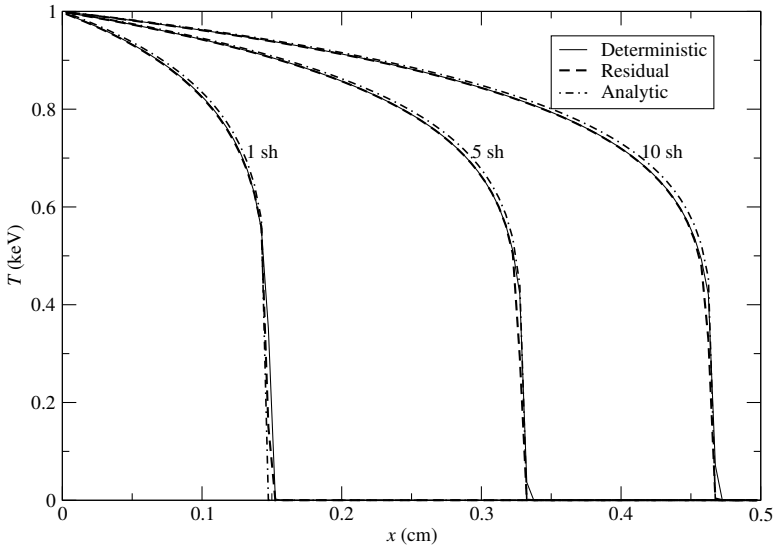

Figure 2. The residual EqDDMC and deterministic solutions to the Marshak wave problem at 1.0, 5.0, and 10.0 shakes.

Figure 2 compares results of the residual Monte Carlo method with the analytic solution to the Marshak problem at 1, 5, and 10 shakes. The residual method results agree well with the analytic solution. Errors between the analytic result and residual result arise because the problem is not spatially resolved enough to account for gradients in the cell-centered diffusion coefficients. The spatial resolution is limited by the restriction on positive probabilities that requires $\Delta x > 4D^n$.

Because of the improved efficiency of the residual method, both in terms of noise reduction and runtime, we can afford to iterate on the non-linearities in the material coefficients. We use the Picard iteration scheme [10] to estimate the material properties at $T^{n+1/2}$ as we convergence on T^{n+1}. The Picard iterations converge on the following condition:

$$\frac{|T_i^{n+1,l+1} - T_i^{n+1,l}|}{T_i^{n+1,l+1}} < \varepsilon, \text{ for } i = 0, \ldots, I, \tag{27}$$

where l is the Picard iteration index. The solutions in Fig. 2 were iterated to convergence using this scheme and a convergence criterion of 0.001. Iterating on material non-linearities is a fully consistent treatment of the non-linearities and, in principle, allows larger timesteps.

As seen in § 4 there are several degrees of freedom in the residual method. Primary among these are the number of particles per stage and timestep. When the timestep is large, the fluxes from the previous timestep may not be good estimates of the new fluxes, and more particles are required to get a good estimate of the residual in the first stage of a timestep. Figure 3 shows a convergence study over timestep and number of particles per stage for the Marshak wave problem. This analysis for relatively small meshes shows that running fewer particles per stage with a smaller timestep is more efficient than running larger timesteps that require more particles per stage. However, running too few particles per stage will result in

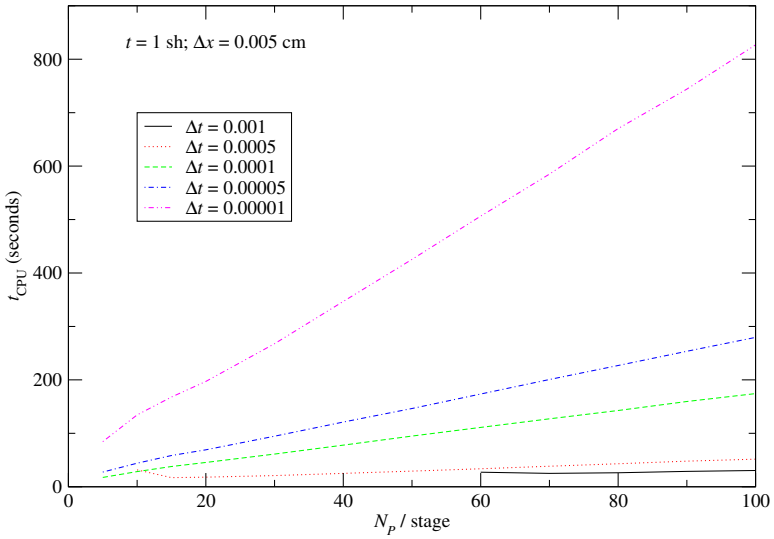

Figure 3. The number of particles per stage versus computer time for 5 different maximum timesteps of the residual method. The Marshak problem was run to a maximum time of 1.0 shakes. The timesteps are in shakes.

an under-sampling of phase space and possibly instabilities and bias, the latter of which is demonstrated in Fig. 4. As shown in Fig. 4, to get good answers at 10 shakes, when there is a lot of energy dispersed over most of the system, the number of particles per stage must be increased to cover the increased amount of discrete phase space.

Figure 4 also shows the advantages of the Picard iterations over using one iteration with material coefficients evaluated at temperatures extrapolated to mid-timestep. This extrapolation is feasible because of the negligible noise in the residual method, but it is not as accurate as Picard iterations. Making this one-pass approach more accurate may involve simply running smaller timesteps. Then the overall efficiency of the residual method is a balance between the cost of Picard iterations and running additional cycles at a smaller timestep.

Because residual methods violate the Central Limit Theorem, the traditional Figure of Merit (FOM) [11] is insufficient for a general error analysis of the residual method. However, we can use the FOM to evaluate a snapshot comparison between the EqDDMC and the REqDDMC methods at a particular time. That is to say, that, if we were to imagine that the residual method converged at a rate of $c/\sqrt{N}$, this evaluation gives us an effective gain of REqDDMC over EqDDMC in the constant c. Figure 5 shows the sample standard deviation of the temperature taken from 30 replicated calculations (each with a different random number seed) of the Marshak wave problem at 1.0 shakes. The sample error is more than an order of magnitude less then the EqDDMC sample error in the wavefront, and it is two to three orders of magnitude smaller behind the wave. For the analog and residual methods Table I shows runtimes, l_∞ norms of the standard deviation of the temperature, and effective FOMs. Clearly, when error and runtime are factored together, the benefits from the residual method are apparent.

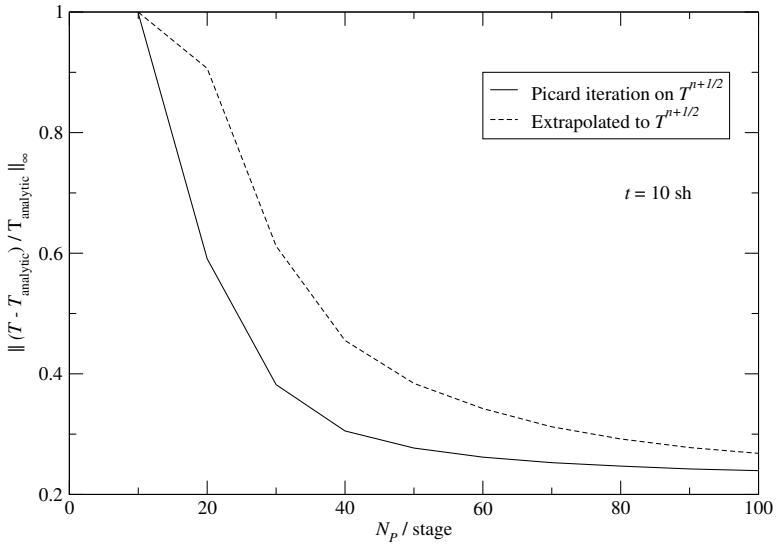

Figure 4. The l_∞ errors between the analytic and residual solutions to the Marshak wave problem at 10 shakes. Both options were run with a maximum timestep of 0.0002 shakes.

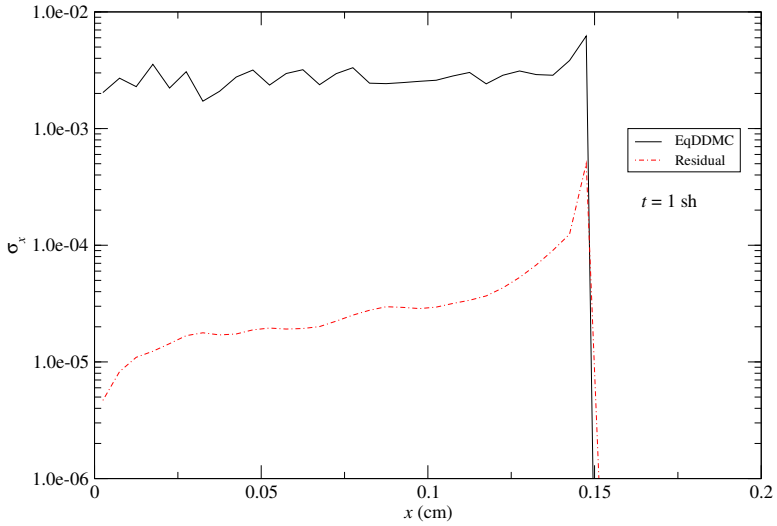

Figure 5. Plot of the standard deviation of the temperature in each cell for the residual and EqDDMC methods on the Marshak wave problem. The Marshak wave was run to 1.0 shakes. Both the EqDDMC and REqDDMC problems were run with a maximum timestep of 0.0001 shakes.

Table I. Runtimes, l_∞ norms of the standard deviation of the temperature, and FOMs for the residual and EqDDMC methods. The sample standard deviations are generated from 30 replicate calculations of the Marshak wave problem to 1.0 shake. Calculations were performed on a LINUX-based Pentium IV processor.

Method	CPU Time (seconds)	$\|\sigma_x\|_\infty$	FOM
EqDDMC	4541.9	6.2×10^{-3}	5.7
REqDDMC	17.0	5.0×10^{-4}	2.4×10^5

Table II. Runtimes of the residual and deterministic solvers on the Marshak wave problem run to 1.0, 5.0, and 10.0 shakes. Both methods utilized identical meshes of 100 cells with $\Delta x = 0.005$ cm. The numbers in parenthesis for the residual runtimes are the number of particles per stage.

		CPU Time (seconds)		
Method	Δt (shakes)	$t = 1$ sh	$t = 5$ sh	$t = 10$ sh
REqDDMC	0.0002	19.44 (5)	269.09 (35)	724.11 (50)
Deterministic	0.001	0.75	2.32	4.16

Finally, given the dramatically improved efficiency exhibited by the residual method over conventional Monte Carlo, we want to compare the REqDDMC method with a deterministic calculation. Table II shows runtimes for the Marshak wave problem run to 1.0, 5.0, and 10.0 shakes for the residual and deterministic diffusion solvers. Both methods iterate on the non-linearities in the material coefficients using the Picard iteration scheme given in Eq. (27). The results are essentially a comparison between the residual method and Gaussian elimination on a tri-diagonal mesh. Gaussian elimination on a tri-diagonal mesh is a $O(2N)$ algorithm; thus, it is very efficient. Figure 2 shows the results of both the residual and deterministic calculations. The residual method results compare very favorably to the deterministic results because there is negligible noise. Although the deterministic calculations are considerably faster in $1D$, we expect that the residual method will be a legitimate competitor to deterministic diffusion in multi-D calculations that require iterative linear solvers. The multi-D results are the focal point of a future study.

Each residual entry in Table II is a separate run with a constant number of particles per stage. As we noted earlier, the Marshak Wave problem requires more particles per stage at late times. Therefore, the overall efficiency of the REqDDMC method could be improved by making the number of particles per stage a variable that starts out small and increases with t. We will analyze methods for performing incremental particle populations in a future study.

6. CONCLUSION

We have demonstrated the application of the residual Monte Carlo method to discrete, non-linear, thermal radiative equilibrium diffusion in one dimension. The residual method shows efficiency gains of several orders of magnitude over the discrete conventional Monte Carlo method on which it is based. The residual Monte Carlo method is successful here because it is applied to a simple discrete system that approximates the continuum diffusion equations rather than the continuum equations themselves. The observed efficiency gains warrant further research into more sophisticated discrete systems that better approximate the continuum equations. Additionally, the success of residual methods on discrete systems warrants a further look at applications to continuum systems.

The residual Monte Carlo method reduces statistical errors to such small levels that it is possible to solve a strongly non-linear, discrete system with a fully implicit treatment of the non-linearities. Although the residual Monte Carlo method is not as efficient as a deterministic method in 1-D, the results presented here

are promising enough to warrant study in multi-dimensional problems. With increasing dimension, Monte Carlo methods generally become more competitive with deterministic methods. The REqDDMC method in multi-dimensions will be the topic of future investigations.

ACKNOWLEDGMENTS

The authors thank Dr. Gordon Olson, Transport Methods Group, Los Alamos National Laboratory, for aid in completing this study. This work was performed under U.S. Government contract W-7405-ENG-36 for Los Alamos National Laboratory.

REFERENCES

[1] J.H. Halton. Sequential monte carlo techniques for the solution of linear systems. *Journal of Scientific Computing*, 9(2):213–257, 1994.

[2] T.E. Booth. Exponential convergence on a continuous Monte Carlo transport problem. *Nuclear Science and Engineering*, 127(3):338–345, 1997.

[3] J.A. Favorite and H. Lichtenstein. Exponential Monte Carlo convergence of a three-dimensional discrete ordinates solution. *Transactions of the American Nuclear Society*, 81:147–148, 1999.

[4] H. Lichtenstein. Exponential convergence rates for reduced-source Monte Carlo transport in [x,μ] geometry. *Nuclear Science and Engineering*, 133:11, 1999.

[5] T.E. Booth. Adaptive importance sampling with a rapidly varying importance function. *Nuclear Science and Engineering*, 136(3):399–408, 2000.

[6] T.E. Booth. An approximate Monte Carlo adaptive importance sampling method. *Nuclear Science and Engineering*, 138(1):96–103, 2001.

[7] J. E. Morel, Todd A. Wareing, and Kenneth Smith. A linear-discontinuous spatial differencing scheme for S_N radiative transfer calculations. *Journal of Computational Physics*, 128:445–462, 1996.

[8] T. M. Evans, T. J. Urbatsch, and H. Lichtenstein. 1-D equilibrium discrete diffusion Monte Carlo. In *Proceedings of the MC2000 - International Conference*, Lisbon, Portugal, July 2000.

[9] A.G. Petschek and R.E. Williamson. Penetration of radiation with constant driving temperature. Technical Report LAMS-2421, Los Alamos Scientific Laboratory, May 1960.

[10] Charles R. Doering and J. D. Gibbon. *Applied analysis of the Navier-Stokes equations*. Cambridge Texts in Applied Mathematics. Cambridge University Press, Cambridge, first edition, 1995.

[11] J. F. Briesmeister. *MCNP-A General Monte Carlo N-Particle Transport Code*. Number LA-12625-M, Version 4B. Los Alamos National Laboratory, 1997.